FEATURE ARTICLE

ChemComm
www.rsc.org/chemcomm

The scanning probe microscopy of metalloproteins and metalloenzymes

Jason J. Davis and H. Allen O. Hill
Inorganic Chemistry Laboratory, Department of Chemistry, University of Oxford, Oxford, UK OX1 3QR. E-mail: allen.hill@chem.ox.ac.uk, jason.davis@chem.ox.ac.uk

Received (in Cambridge, UK) 7th September 2001, Accepted 23rd November 2001
First published as an Advance Article on the web 1st February 2002

In recent years, the concept of microscopy and the ability to study processes at a truly molecular level have been revolutionised by the development of a family of instruments based on acquiring data through the scanning of a proximal probe across a surface. Scanning Probe Microscopes (SPMs) enable surface-confined structures to be resolved at ångstrom-resolution, in real time, and under a variety of controllable conditions. Despite initial difficulties, much progress has been in the application of this technology to the high-resolution analysis of biological systems; these have varied from complex cellular systems to molecular biopolymers. Studying the interactions of protein with surfaces has been intrinsic to the development of our understanding of blood coagulation, fibrinolysis, thrombus formation and the synthesis of biocompatible materials. The specific interactions of metalloproteins and enzymes with electrode surfaces remains central to the understanding of the bioelectrochemical processes and to the development of biosensing devices. Though ellipsometry, Raman, microcalorimetry, surface plasmon resonance, and other spectroscopic methods, can provide much information on these interfaces, the acquired data are averaged over a large number of molecular species with a low spatial resolution. Proximal probe methods have much to offer in this regard and have revolutionized our ability to monitor such interactions.

Jason John Davis was born in London in 1971 and attended Kings College London where he received several prizes and a BSc in Chemistry in 1993. His doctoral research on bioelectrochemical interactions, carbon nanotubes, buckminsterfullerene and scanning probe microscopy was conducted at the Inorganic Chemistry Laboratory in the University of Oxford under the supervision of Professor Allen Hill. He was awarded a DPhil in Chemistry, an Extrordinary Junior Research Fellowship at The Queen's College in 1998 and continued postdoctoral studies with Allen Hill until 1999 when he was awarded a Royal Society University Research Fellowship. His current research interests focus on molecular-level biological and chemical studies as well as biological electron transfer processes.

Allen Hill is Professor of Bioinorganic Chemistry in the University of Oxford. He began his career as an organic chemist, and then studied the reactions of vitamin B_{12} and the physical properties of bioinorganic 'model' complexes. In the late 1960s, he realized that methods were becoming available to investigate the structures of proteins and enzymes so he began to study the NMR of copper proteins and enzymes. Recognizing that the direct electrochemistry of redox proteins had not been reported, he found a way of achieving this which led to the discovery of a new electrochemical method of analysis which gave rise to a commercially successful glucose sensor. He now concentrates on the SPM of biological entities and, with colleagues, has started a company, Oxford Biosensors, to exploit microarray electrodes. He was elected a Fellow of the Royal Society in 1990 and received the Mullard Medal in 1993.

The two processes central to sustaining life on earth, respiration and photosynthesis, involve electron transfer reactions of metalloproteins and metalloenzymes. If one is able to generate a suitably bio-compatible interface, it should be possible to persuade such entities to communicate with man-made circuits. Bioelectrochemical studies, during the past 20 years or so, have provided information central to both enhancing our understanding of electron movement in biology and to the generation of (electrochemically-based) biosensing devices. For example, glucose sensors are of great use to those unfortunate enough to have diabetes. Commercially available sensors contain the enzyme glucose oxidase irrespective of the method of transducing the information, though those based on electrochemical techniques have grown in popularity. The ferrocene-based glucose biosensor, born out of such studies,[1] led to the creation of Medisense Ltd and the fabrication of a device responsible for improving the lives of countless diabetics worldwide. Though highly-effective, the enzyme–surface interface within these devices is poorly understood and formed by processes which are not controlled at a molecular level. The activity of immobilized enzyme is easy to assess; what about the structure or arrangement of these molecules on the electrode surface? Recent technological advances have allowed this interface to be refined to one at which *individual* glucose oxidase molecules can be 'visualized' under conditions in which they are functionally-active [Fig. 1]. What useful information can such studies provide? In what way do the images apparent correspond to the 'true' biological structure? What are the possibilities and limitations of this technology? These are questions that we will attempt to address.

Scanning probe microscopy

Atomic Force Microscopy (AFM), probably the most versatile and commonly used of the scanning probe family, generates three-dimensional images of a surface in much the same way as the needle of a record player senses the grooves of a record. This 'needle', or tip, is, however, atomically-sharp and attached to the terminus of a highly sensitive cantilever (with a spring constant less than the equivalent constant between atoms in a solid). As the probe tracks across a surface, the forces it experiences (both attractive and repulsive) are translated into vertical deflections of this lever. These movements are in turn monitored with exceedingly high accuracy with a laser beam; a typical 'beam deflection' system is able to detect laser movements of less than 0.5 Å.

DOI: 10.1039/b108128b

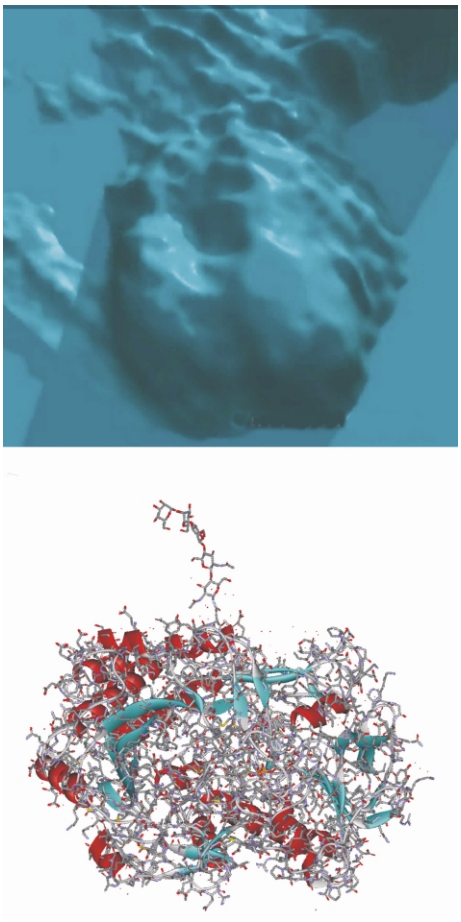

Fig. 1 STM image of a single glucose oxidase molecule immobilized on an anodized HOPG electrode surface under 20 mM potassium phosphate buffer, 10 mM KCl (image size 20 × 20 nm). With convolution, the molecular dimensions of the glycosylated enzyme, as determined by tunnelling, are in reasonable agreement with those predicted on the basis of the published[55] de-glycosylated crystal structure (shown).

One crucial development in the application of AFM to relevant biological systems was the realization that biological samples could be analysed at high resolution under solution; that is, in an environment which can closely approximate the physiological. This contrasts strongly to the high vacuum characterization of dehydrated or frozen hydrated (and often stained) samples by electron microscopy. Not only are samples retained in a more native state, but it is possible to carry out their characterization in a notably less destructive way; samples are not, for example, bombarded with high energy electrons. As a consequence of this ability, it is possible to monitor dynamic biological processes as they occur in real time at a truly molecular level. In addition, though three-dimensional data sets can be obtained from inherently two-dimensional electron microscopy projections of sample specimens by sample tilting, this can be cumbersome and of somewhat limited applicability. The vertical resolution consequently obtained is often low. In stark contrast, scanning probe methods, by their very nature, produce three-dimensional information and can offer exquisite (sub-ångstrom) vertical resolution. Of perhaps even greater significance, and in contrast to practically all other methods of characterizing and analyzing biological structure, these methods produce data of a truly molecular nature. The gross averaging of molecular characteristics inherent in diffraction or spectroscopic (including NMR) methodologies is totally absent. In summary, the ability of these methods to produce molecular-level unaveraged biological structural data presently surpasses that of any alternative.

Perhaps the most major challenge associated with undertaking any biological scanning probe experiment lies in developing a non-destructive method of anchoring the molecules of interest to the chosen, often atomically-flat (surface roughness significantly smaller than the vertical height of the molecules) substrate. This immobilization procedure is a delicate balance; it must be sufficiently strong for molecules to be both diffusionally-inhibited and stable under the forces imparted by the scanning (sensing) probe but not so strong that natural structural integrity is lost (largely negating the usefulness of subsequently obtained data). In the past 3–5 years progress has been made in covalently tethering biomolecules by either chemical modification of the underlying substrate surface[2,3] or of the biomolecule itself.[4] These methods have been successful but a more controlled, site-specific, tethering method offers considerable advantages, especially in terms of controlling molecule–electrode electronic coupling (see below).

Biological atomic force microscopy

Soft, compressible, samples are often unreliably imaged (if at all) under the shear forces typically present under contact mode imaging conditions. In order to facilitate the imaging of these delicate specimens, advances in this imaging method, in which the probe is effectively dragged across the surface of the sample, were sought. These have all focused on dramatically reducing the lateral forces imparted to the surface molecules by the scanning probe and include non-contact and intermittent contact methodologies, the most demonstrably successful being 'Tapping Mode' (TMAFM). In TMAFM [Fig. 2] the shear problem is greatly reduced by periodically 'tapping' (at high frequency) the surface with the tip as the two scan relative to each other. The cantilever is driven at, or near to, its resonant frequency by the acoustic wave generated by a piezoelectric crystal.[5,6] Importantly, the tip makes transient contact with the sample only at the bottom of each oscillation—the lateral forces inherent in contact scanning are, thereby, eliminated. Energy dissipated between the contacting tip and surface at this point leads to a change in the oscillation amplitude during scanning. This (nm scale) change in amplitude serves as the feedback signal and is used to generate topographic images. The magnitude of lever energy dissipated depends on both scanning conditions and the mechanical properties of the sample. Oscillation phase changes can additionally be measured and related to surface adhesion, friction and viscoelastic properties.[7,8] More recently, a greater level of control over the tip–sample interaction has been achievable through the use of magnetically coated AFM levers, driven at low oscillation by an alternating magnetic field.[9,10]

Biological scanning tunnelling microscopy

A scanning tunnelling microscope consists, in essence, of a low current amplifier, a sample positioning stage, a scanning unit, feedback electronics and a computer system for control, data acquisition and display. A small voltage (typically several hundred mV) is applied between the proximal probe (for example 0.25 mm diameter platinum wire) and the sample/substrate surface. The two electrodes are then brought slowly together until their (sub nanometer) separation is such that electrons can tunnel through the classically impenetrable barrier between them. The tip and substrate are then scanned precisely relative to one another and the current accurately monitored as a function of position. In order to monitor low tunnelling currents in solution, it is necessary to effectively insulate the probe from (largely) capacitative current flow. This is most commonly achieved by a careful immersion of etched probes into molten wax. As solution conditions move closer to physiological and ionic strengths increase, so this process becomes more demanding. The interested reader may wish to consult, amongst others, references 27, 31 and 32 for further experimental detail.

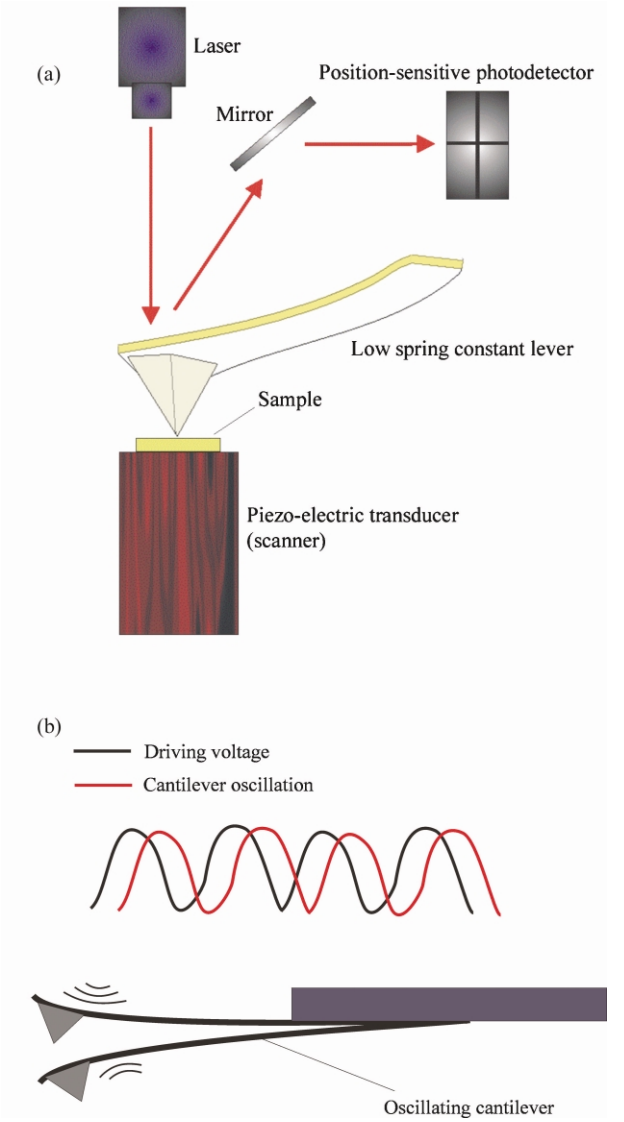

Fig. 2 (a) Diagrammatic representation of the basic components of an Atomic Force Microscope. Relative, precise, lateral sample-lever movement is achieved by mounting either the sample or the lever itself on the end of a piezo-ceramic material—the scanner. A laser beam is focused onto the back of the cantilever, reflected onto a mirror and finally onto a position-sensitive photodiode. By monitoring beam movement across the photodiode as tip and sample scan relative to each other, a three-dimensional image of the surface is generated. Such an 'optical-beam' set-up is capable of detecting lever deflections considerably less than 1 Å in magnitude. (b) Tapping Mode AFM imaging; a sinusoidal voltage is applied to a piezo crystal and used to generate an acoustic wave. This wave drives the cantilever into KHz oscillation. Changes in the (offset) sinusoidal movement of the reflected laser, as monitored by the photodetector, are used to generate the surface image.

On account of the lower tip contact area (see below) with the sample, STM methods offer, in theory, an inherently higher resolution than AFM (operated under normal conditions). Since most biomacromolecules are[11] electrically insulating (resistivities typically 10^{15}–10^{18} Ωm), the applicability of STM was, however, originally (and to some extent still is) regarded to be very limited. The major difficulty lies in the fact that the atomically-sharp tip will depress the molecules until the set-point current flows between it and the underlying substrate surface. The forces imparted during this process are difficult to control or quantify but have been estimated, under some conditions, to be as high as 100 nN. Early studies focused on coating the sample with electrically-conducting Pt/C or Pt/Ir/C films, though this process prevents the direct observation of either native structure or dynamics; it has since been shown to be both unnecessary and detrimental to resolution of native biological structure. Other studies have focused[12] on imaging under conditions of very high tunnelling resistance.

The measured current is precisely modulated by the presence of adsorbates present in this tunnelling gap. Under conditions of normal bias, electrons are assumed to tunnel from tip to substrate (or *vice versa*) and not to accumulate on the molecules in the gap or to interact significantly with molecular states.[13] Though the details of the mechanisms involved in this process lie beyond this review, adsorbate-induced modulations in surface work function and/or density of states are likely to play a role in most cases.[14,15] The tunnelling profiles of large band gap molecules, in which the HOMO and LUMO are several eV away from the metallic Fermi levels, cannot be easily accounted for. The means by which biomolecules, in particular, are imaged by STM is a subject of much debate and we would direct the interested reader to recent articles by Lindsay and Ulstrup.[16,17] Since the direct tunnelling through an adsorbed protein, for example, would involve typically distances of at least 30–50 Å, (assuming little structural deformation), this has posed a considerable theoretical problem.

Some studies have suggested that tunnelling images are more easily obtained[18] under conditions of high humidity. Guckenberger *et al.*, for example reported[19] successful imaging of the hexagonally packed intermediate layer (HPI) from the bacterium *Deinococcus radiodurans* only at humidity levels of 40% or more, though successful studies have also been carried out at ambient or poorly-defined conditions of humidity. Ulstrup *et al.* have discussed,[17,20] in detail, the mechanisms of resonance-enhanced tunnelling through metalloproteins but, to date, this has not been demonstrated with any biological system. In summary, due largely to the complexity associated with simulating the process of electron tunnelling through a large, fluxional biomolecule, its complex electronic structure, and indeed the influence of adsorption on this, there is currently no single mechanism which can explain[16,21] the image contrast generated. Despite this, a number of groups have reported the successful imaging of protein or enzyme molecules by STM. These have included cytochrome *c*,[22] cytochrome *c*551,[23] phosphorylase *b* and phosphorylase kinase,[24] glucose oxidase,[25] catalase,[26] azurin,[27,28] haemoglobin,[29] rubredoxin,[30] metallothionein[31] and cytochrome P450cam.[32]

STM and AFM studies

Azurin

Azurins are[33,34] well-characterised type I or blue copper proteins which function as electron transfer mediators at positive potentials. The small (10–15 kDa) metalloproteins contain a single copper atom strongly asymmetrically located in a hydrophobic core approximately 7 Å from the surface. The controlled introduction of specific residues into the protein primary structure by site-directed mutagenesis has led to the production, characterization and utilization of a number of mutants in recent years.[35,36]

The physical (non-covalent) adsorption of proteins at solid interfaces is governed by a complex interplay of (primarily) electrostatic, hydrophobic and dispersion forces. Voltammetric investigations of redox proteins have largely focused[37] on tailoring the electrode-solution interface such that these interactions are more biocompatible. Many self-assembling thiol or disulfide-based molecules, for example, provide a suitable interface with which proteins will interact reversibly and non-destructively (proteins typically unfold on bare noble metal surfaces). Few studies have, however, attempted to directly control protein surface orientation. Several years ago, we investigated the controlled immobilization of azurin molecules on gold electrodes through introduced surface cysteine residues (utilising the strong gold–thiol covalent interaction—L-cysteine itself, is known to bind strongly to gold *via* the thiol functionality).[32,38] On incubation of single-crystalline (Au

[111]) electrodes in dilute solutions of this protein, well-defined monolayers could be obtained which were stable to repeated scanning (under buffered solution) by both AFM and STM [Fig. 3]. These adlayers are commonly sufficiently stable for

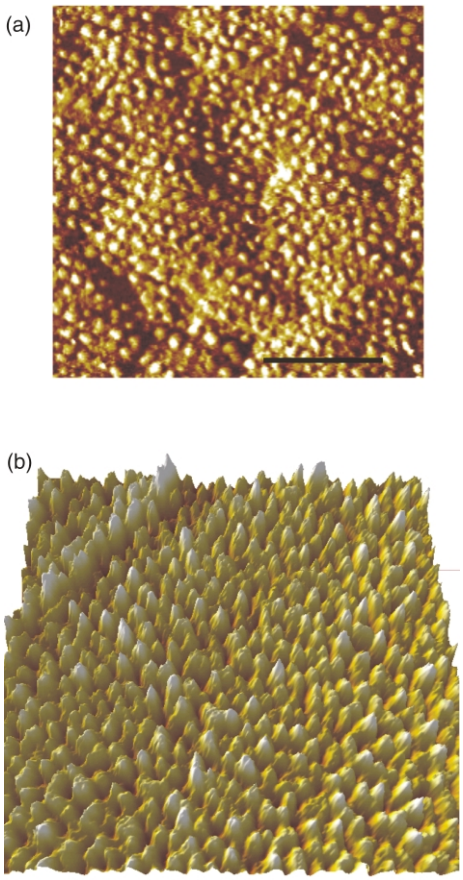

Fig. 3 (top) Tapping Mode AFM image of an immobilized azurin monolayer under 15 mM potassium phosphate buffer, pH 7. Scale bar 300 nm. (bottom) Tunnelling image of a similarly-formed monolayer under buffered solution. Image size 140 nm × 140 nm. The lateral dimensions of the molecules within this image are 4–5 nm, close to the expected molecular size and indicative of minimal convolution.

individual, isolated molecules (free from the stabilizing lateral interactions inherent in a packed monolayer) to be identified [Fig. 4]. These structures are measured at 4–4.5 nm in diameter

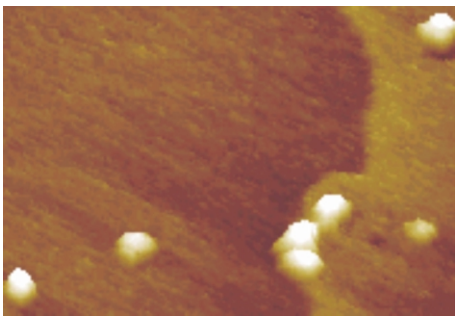

Fig. 4 Fluid tunnelling image of individual, isolated azurin molecules on a gold electrode. Image size 50 nm × 30 nm. This image, taken from an *in situ* time-resolved experiment, is that obtained approximately 30 min after the injection of 100 μl of 100 μM solution of an azurin surface cysteine mutant.

by STM (the blunter tip inherent in AFM produces convoluted measurements); the long axis of the azurin molecule is approximately 3.5 nm in length. The exceptional vertical resolution of an AFM can be utilized in measuring the heights of these immobilized molecules. The data obtained are centered at a value very close to that expected with the protein anchored through the introduced surface residue [Fig. 5]. This is also

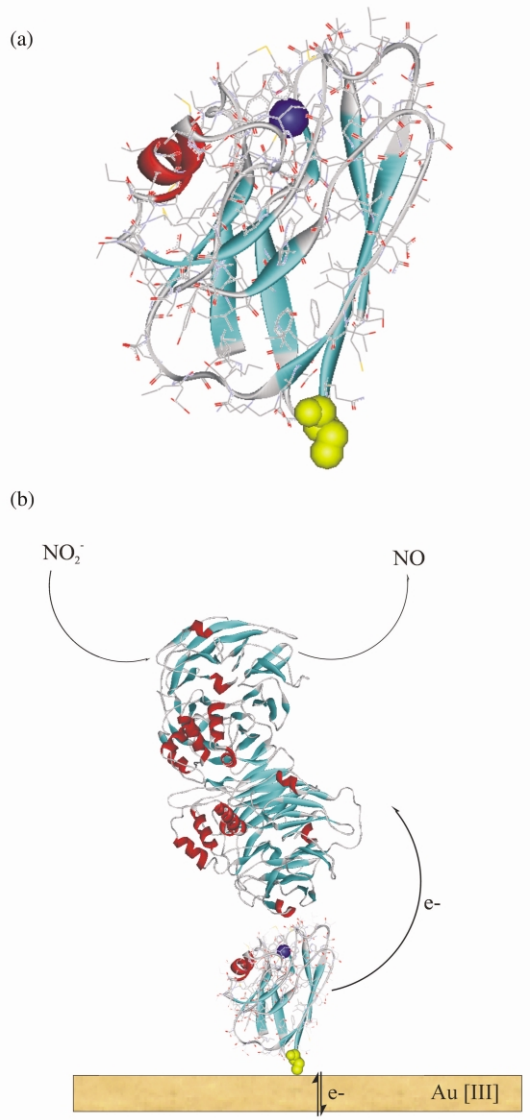

Fig. 5 (a) Graphical representation of the structure of *Pseudomonas aeuruginosa* azurin K27C. The copper center is highlighted in blue, the introduced surface cysteine residue in yellow. (b) Schematic of a possible electron transfer relay at the electrode surface. Note: the reductase is[56] illustrated in its dimeric form and in arbitrary orientation.

consistent with a non-denaturing immobilization, non-destructive imaging and electrochemical data obtained with the same protein. Studies carried out with the wild-type protein are consistent with immobilization *via* the exposed disulfide (Cys3–Cys26) moiety. This is an integral part of the protein structure and presumably undergoes at least a partial cleavage at the surface. Perhaps unsurprisingly then, height measurements with the wild-type protein are consistent [Fig. 6] with a significant population of a denatured, 'low height' form. The electrochemical response obtained from such a system is transient. Studies such as this allow us to engineer the physicochemical and electronic interactions of metalloproteins with surfaces, and to monitor such in real time and at a truly molecular level[27,32] By monitoring the process of azurin molecular adsorption, it is possible to demonstrate, as it similarly is with a number of other protein–substrate systems, an expected preferential adsorption at surface sites of higher free energy *i.e.*, step edges and defects.

If one is able to generate bioelectrochemical interfaces with this level of control and analysis, it may be possible to build up, stepwise, natural biological electron transfer relays at surfaces.

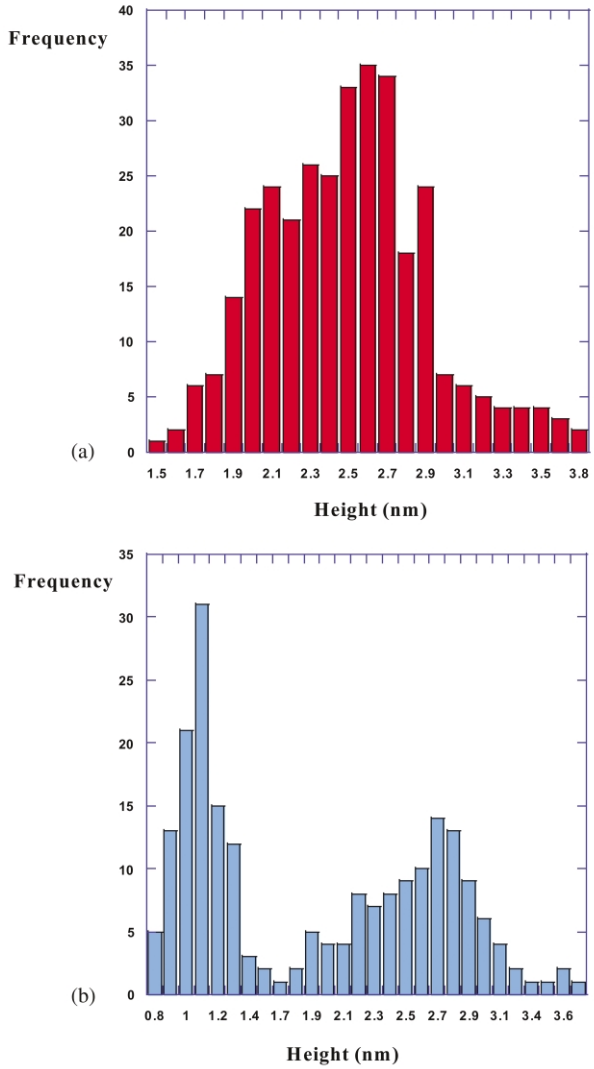

Fig. 6 Statistical analysis of the azurin K27C molecular height distribution as measured under buffered solution (a) and in comparison to that observed with the wild-type protein (b).

An example of such is shown in [Fig. 5(b)]. Azurin molecules are anchored at the terminus of the structure such that the natural (hydrophobic) binding site, close to the copper, is exposed. One can then envisage that its natural partner, the enzyme nitrite reductase cd1 will bind, at least transiently, to this site, turn over any nitrite substrate present in solution, and exchange electrons with the azurin. If the copper protein is itself electronically-coupled to the underlying electrode surface, this substrate turnover will be quantitatively detected. Provided the structures at the interface are sufficiently robust, it may be possible to monitor, in real-time, the assembly and dynamics of such 'molecular' nitrite biosensors by scanning probe methods. Studies with this aim are presently underway at Oxford.

Functionally-active glucose oxidase molecules

Glucose oxidase (β-D-glucose:oxygen 1-oxidoreductase), a 160 kDa glycoprotein containing two identical polypeptide chains, catalyses the oxidation of β-D-glucose to D-glucono-1,5-lactone and hydrogen peroxide, using molecular oxygen as the electron acceptor. Importantly, glucose oxidase can use a number of artificial electron acceptors in its redox reaction (other than dioxygen as the electron sink). By linking this redox process to man-made circuitry, it is possible to utilise the efficiency of this enzyme in turning over glucose in the generation of glucose biosensors. Some twenty years or so ago, the ability of ferrocene and its derivatives to 'mediate' the communication between electrode surfaces and the catalytically-active redox site of the enzyme was[1] demonstrated. This subsequently led to the development of the glucose biosensor (now marketed world-wide by Abbott Inc.)

The Highly Orientated Pyrolytic Graphite electrode surfaces commonly used in scanning probe experiments is highly uniform, hydrophobic and far from biocompatible. By partially oxidizing such a surface (chemically or electrochemically), however, it is possible to create arrays of hydrophilic (oxygen-moiety-functionalised) sites on which enzyme molecules can be preferentially adsorbed. In an *in situ* electrochemical STM experiment, it is possible to not only resolve the gross structure of these enzyme molecules, but also to simultaneously probe their activity. Fig. 1 is a high resolution tunnelling image of a single enzyme molecule in which the dimeric 'butterfly' structure is resolved under buffered electrolyte. Though the exact fluid dimensions of the enzyme from *Aspergillus Niger* (as used in this study) are unknown, it is likely to be close to 10 nm across[39]—the relationship between the crystallographically-defined de-glycosylated structure and that observed with a glycosylated molecule confined to a surface under fluid is unknown. With convolution, the molecular dimensions as determined in this tunnelling study, are in good agreement with those predicted. A catalytic electrochemical response can be simultaneously obtained on the addition of ferrocene mono-carboxylic acid and glucose substrate; though not molecularly resolved, this does at least demonstrate that native structure–activity under these experimental conditions, is largely re-tained.

Tunnelling through Zn_7 metallothionein

Contrast in adsorbate STM images has been found to be dominated by topography unless electronic effects are strong. This arises largely because of the extreme sensitivity of the current to minute changes within the confines of the tunnel gap; when the tip scans over 'high' regions of a molecule, the current transiently increases since the tunnelling decay coefficient through the structure is likely to be less than that of the 'empty' (vacuum, air or fluid filled) gap—this leads to 'positive contrast' in that the adsorbate appears (correctly) to be higher than the substrate surface on which it sits.

One could postulate that, with a protein in which the metal content is high in terms of its molecular size, resolving submolecular tunnelling contrast, due to metal-related electronic effects, was a reasonable possibility. In a study of Zn_7-metallothionein (seven heavy-metal atoms in a protein of only sixty amino acids) on gold, a striking pattern of enhanced contrast was[31] observed in fluid STM imaging [Fig. 7]. The gross 'dumbell' structure of the protein was resolved but, more interestingly, a comparison to a simplified representation of the crystal structure reveals a very close correspondence between the positions of enhanced contrast and the expected positions of the metal centers. The '2 × 2' and '1 × 3' zinc centres appear to be resolved as regions of high tunnelling conductance. This may be due to the ability of spatially-extended d-orbitals to facilitate tunnelling though the contributions of the sulfur-based ligands (of which there are twenty) to this contrast cannot[40] be ruled out. Experiments such as these not only contribute to our understanding of protein–surface interactions, but also provide a very direct, molecular-level approach to the analysis of charge transport through a protein matrix.

Characterisation of P450cam enzyme adlayers

Of the many enzymes known to catalyse redox reactions involving molecular oxygen, the *b*-haem-containing cyto-chrome P450 monooxygenases have attracted much attention. These enzymes are widely distributed in nature, able to catalyse the controlled activation of dioxygen and play a role in the biosynthesis of steroids, drug metabolism, the bioactivation of polycyclic aromatic hydrocarbons (PAHs) to carcinogens, and

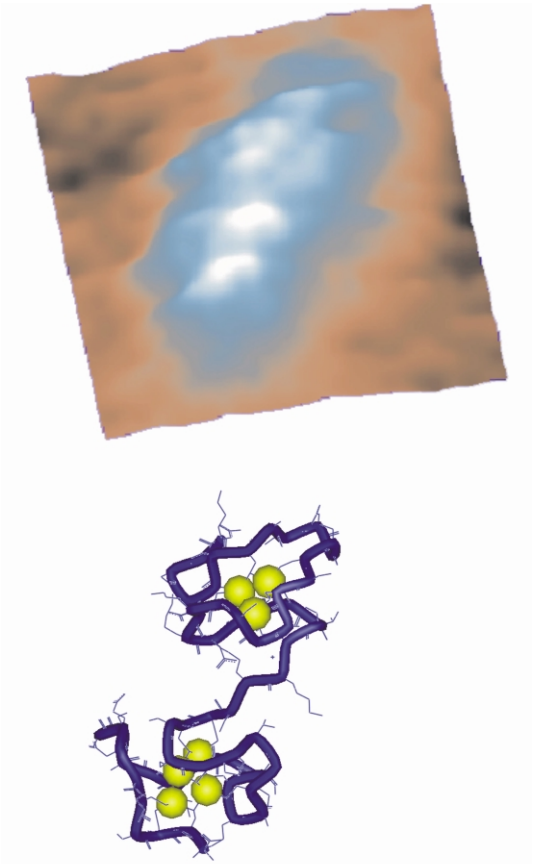

Fig. 7 Comparison of a STM image of a single Zn_7-metallothionein molecule adsorbed on a gold electrode surface under potassium phosphate buffer with the protein structure as determined by diffraction. Note the apparent strong correlation between regions of high tunnelling contrast and the expected positions of the heavy metal centres. Image size 3 nm × 3 nm.

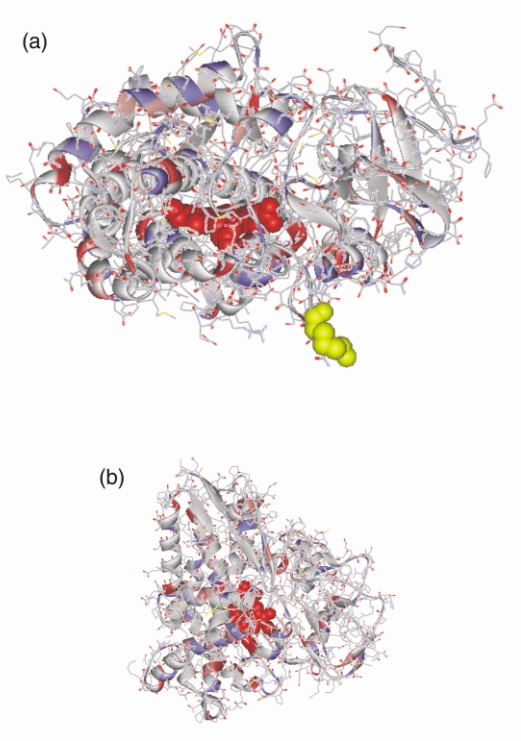

Fig. 8 Computer generated representation of the crystallographically determined structure of cytochrome $P450_{cam}$. The structure is presented (a) with the K27C surface cysteine highlighted and orientated face-down. The haem moiety (also highlighted) is approximately 10 Å from the lower face of the enzyme. The structure is viewed from above (the 'tip-view') in (b).

blood detoxification. In recent years, much effort has been put into obtaining[41,42] reliable voltammetric responses from the (buried) enzyme haem group. If this can be achieved, with the enzyme immobilized in a redox-addressable, active form, one can postulate the generation of derived biosensing systems targeting specific compounds in the environment.

Cytochrome $P450_{cam}$ from *Pseudomonas putida* is a stable member of the P450 family and catalyses the regio- and stereospecific hydroxylation of camphor to 5-*exo*-hydroxycamphor. Progressing from the methodologies outlined above, it is possible to use a site-specifically engineered surface cysteine residue to both create well-defined molecular adlayers, of high stability and, perhaps more importantly, to control the electronic coupling between the enzyme and the underlying gold electrode surface. This enzyme contains eight cysteine residues in its wild-type form, five of which are at, or near to, the protein surface; in order to carry out the immobilization in a specific orientation, these five residues were replaced by chemically inert alanines. A cysteine residue was then introduced into position 344 (replacing a lysine to produce a K344C mutant). This site resides within a patch on the enzyme surface thought to be involved in interactions with its native redox partner, putidaredoxin[43] and in a region of the enzyme where the haem is closest (approximately 10 Å) to the surface[44] [Fig. 8(a)].

As with analogous studies with azurin, incubation of pristine gold electrodes surfaces in dilute solutions of this enzyme leads to monolayer coverage which is nicely resolvable in ambient tunnelling studies [Fig. 9(a)]. More reproducibly ordered adsorption is observed with this mutant, than with the wild-type enzyme. At higher magnification [Fig. 9(b)], a significant number of molecules appear to have a recognizable 'triangular' shape. On reference to graphical representations of the enzyme, with the introduced surface cysteine assumed to be 'face down' on the gold, one indeed expects such a shape [Fig. 8(b)]. Though one does not necessarily expect the molecular dimensions of a surface-confined hydrated enzyme to mirror those derived from diffraction methods, tunnelling images generated under fluid were, in general, within 20% of crystallographic dimensions; X-ray studies have suggested that cytochrome P450s have a triangular prismatic shape, approximately 6.5 nm on each side and 3.5 nm thick.[45] Interestingly, images obtained under ambient atmosphere gave molecular dimensions of, on average, 7–8 nm × 8–9 nm, though one would not expect tip-based convolution effects to be reproducibly greater under these conditions. It is possible that, under typical ambient conditions, a significant proportion of the tunnel current is carried by a thin film of water present on the surface of the molecule.[16,46] The contribution of protons to the image current has been demonstrated in the case of both water and methanolic atmospheres, where a reduction in humidity can result in a drop, or even a reversal, of image contrast.[47] Since current does not flow through the protein under such conditions (only over its surface), only the gross structure is resolved.[48] Several recent tunnelling studies carried out in solution have, however, been able to resolve internal protein structure and, consequently, tunnelling must occur through the structure when it is immersed under these conditions.[28,30,31] It seems reasonable to propose that the presence of a hydration layer around the enzyme molecules in ambient atmosphere may be responsible for somewhat magnifying the molecular dimensions.†

Getting the enzyme to exchange electrons with an underlying electrode surface is somewhat difficult due largely to the buried nature of the haem prosthetic group. With the K344C mutant, however, this electronic coupling (on a bare, single crystalline gold electrode) is strong, consistent with the enzyme being anchored down through the face at which the haem is closest [Fig. 8(a)]. One can accordingly postulate that there exists a facile tunnelling route through the protein matrix, along which lies the haem moiety. Furthermore, activity assays demonstrate

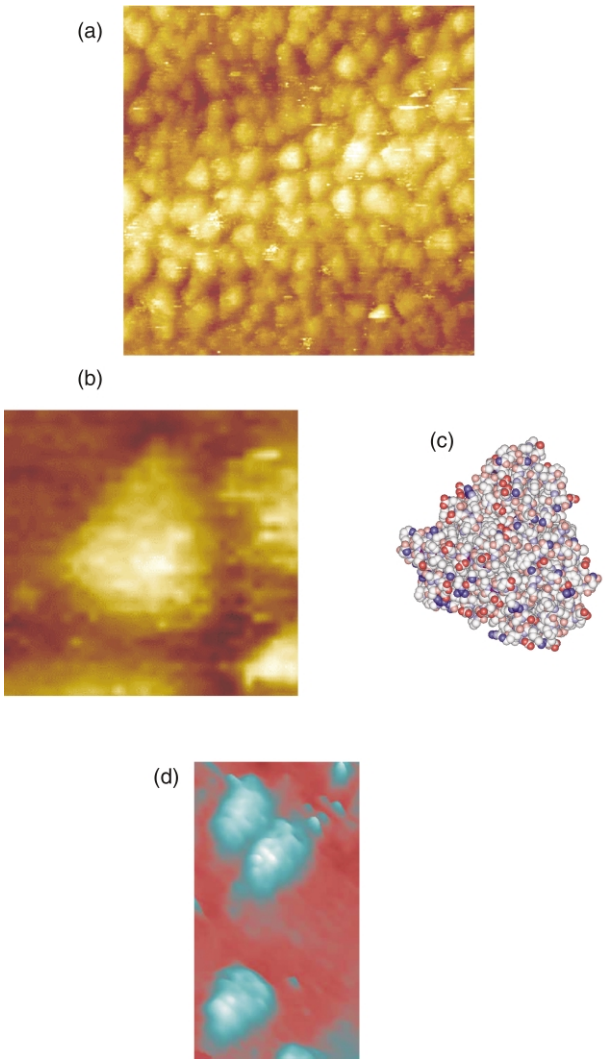

Fig. 9 (a) Ambient tunnelling image of an immobilized cytochrome $P450_{cam}$ mutant adlayer on a single crystalline gold electrode surface. A complete monolayer coverage is evident. These molecules are electrochemically coupled to the underlying gold electrode surface. Scan size 90 nm × 90 nm. (b) Ambient tunnelling image of a single immobilized enzyme molecule. An orientated space-filling crystallographic representation of the structure is shown on (c) for comparison. (d) Fluid (under potassium phosphate buffer) tunnelling image of three enzyme molecules.

the enzyme adlayers largely retain their activity under such an immobilization procedure. As with azurin, studies such as this, in which the enzyme is anchored to surfaces in well-defined arrays, can be extended to those in which specific (perhaps redox) interactions with natural partners are monitored at a molecular level. Studies with the iron–sulfur protein, putidaredoxin are underway to this end.

Though the greater tip-sample contact area of AFM studies result in images of a somewhat lower lateral resolution, under conditions of negligible (checked by monitoring the effect of operational forces on measured data) compression, the height data are exceedingly accurate (to less than one ångstrom if the instrument is reliably calibrated). In using this fact and deconvoluting tip contributions to lateral data, molecular volume determinations can be fairly reliably executed by AFM. With the $P450_{cam}$ adlayers above, such measurements produce a value of 68 nm^3 on average. If one approximates the molecule as spherical for this purpose and assumes a molecular density of 1.14 g cm^{-3} (0.4 mol of water per mol of enzyme) we arrive at a figure in the range of 60–70 nm^3.

Despite the difficulties associated with the need to balance potentially destructive probe–biomolecule interactions with the need to produce high-resolution imaging, both AFM and STM methodologies can lead to a molecular-level resolution of (even very small) biomolecular systems. Further to this, with appropriate two-dimensionally ordered samples and the application of the advanced image processing methods common in electron microscopy, biomolecular interfaces can be resolved with resolutions in the sub-nanometre range.[49,50] Shown in Fig. 10 is a high-resolution AFM image of the ATP-powered,

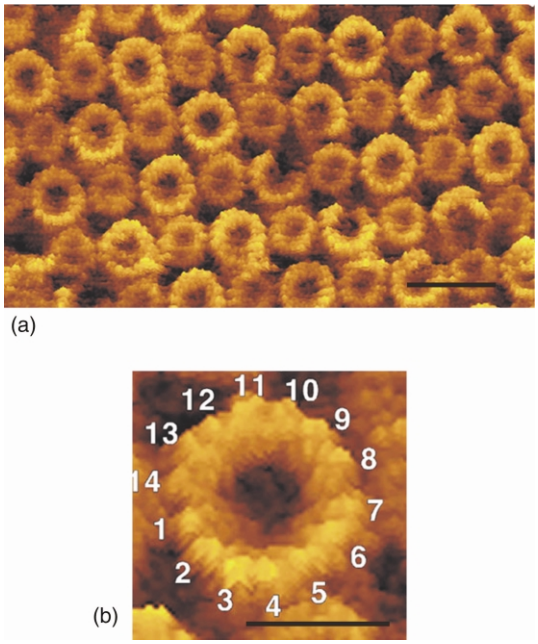

Fig. 10 Contact AFM image of chloroplast ATP synthase oligomers. Reproduced from reference 50. Scale bars 10 nm (a) and 5 nm (b). The 14 constituent subunits are evident in (b). Z-range 0–2 nm. (Reproduced with permission from *Nature*,‡ 2000, **405**, 418–419, copyright (2000) Macmillan Magazines Ltd.)

membrane spanning motor, ATP-synthase (chloroplast) in which the 14 protruding symmetrically-distributed subunits are resolved under buffered aqueous solution.[50]

Resolution

Each pixel in an AFM or STM image is representative of a measured cantilever deflection or amplitude (AFM) or tunnel current (STM). Under normal AFM operational conditions, with standard probes, these are brought about by the summed interactions of tens-to-hundreds of atoms. The contact area in STM experiments is typically smaller but the compressive interactions are more difficult to control or quantify. This tip-sample contact area depends upon geometric and mechanical considerations and represents a resolution limitation. Though these methods are undoubtedly powerful in allowing visualization of single small biomolecules under quasi-physiological (and electrochemical, if appropriate) conditions, resolution is not often reproducibly sufficient to resolve anything more than gross quaternary structure (1–2 nm). With biomolecules, convolution problems are further aggravated by both structural motion inherent in the hydrated structure and tip-induced compressional changes. Though we continue to make progress in reducing these problems, in order to learn more about the scanned structure–activity, it will be necessary to marry topographic/electronic imaging to simultaneous spectroscopic analyses. During the last decade very considerable advances in optical microscopy have been made. Confocal and total internal reflection fluorescence methods, in particular, have been impressively applied to biomolecular analyses. Though, to date, biological samples have been characterized at a molecular scale

only with considerable difficulty, near-field scanning optical microscopy (NSOM) has emerged as a particularly powerful and versatile combination of scanning probe and optical technology. These constantly improving technologies bring us, yearly, closer to the ability to monitor topographic, electronic spectroscopic and dynamic properties of individual biological molecules.[51,52]

Summary and conclusions

SPM can make a very significant contribution to the analysis of protein/enzyme–surface interactions. High signal : noise images can be obtained under physiologically-relevant conditions and processes monitored in real-time.[27] A detailed understanding of these interactions remains valuable in clinical diagnostics (such as biosensor fabrication) and the development of biocompatible materials. AFM images of hydrated biological structure can now be obtained with reasonable ease.[53] Though the absence of a direct control of tip-sample interaction forces means that tunnelling imaging remains far from straightforward, several research teams worldwide have, however, persevered with these largely because they offer not only greater lateral and vertical (if not 'real') resolution, but also give one the ability to resolve tunnelling pathways through *individual* molecules; the process of electron tunnelling in chemical and biological systems is of very considerable importance and has been studied experimentally and theoretically in much detail. STM imaging provides a *direct* means of associating tunnelling behaviour with specific environmental and molecular parameters. In recent years, data have been produced with a sufficiently high resolution to resolve sub-molecular tunnelling features; for example, a differential high tunnelling contrast has been noted in images of heavy-metal-containing metallothionein molecules and the blue copper protein, azurin.[27,32] In the STM configuration, regions of greater contrast correspond to those where tunnelling probability (tip-to-sample *via* molecular adsorbate) is greater. It is possible that facile tunnel routes through the protein matrix, namely those on which the metal center lies, are being detected. Under normal imaging conditions, however, one would perhaps expect that structural fluctuations (natural or tip-induced) would lead to any image being representative of averaging over many possible tunnelling pathways. Though a detailed interpretation of these current contrast profiles is lacking they are undoubtedly indicative of the ability of STM to resolve *internal* (electronic) structure within these hydrated biomolecules. The ability to carry out such studies under full electrochemical control means that data can be acquired with an unrivalled level of control over the relative energies of orbitals which may be responsible for mediating tunnelling. The control and analysis of tunnelling through a single molecule has been strikingly demonstrated with metalloporphyrins.[54] Attempts are underway to achieve the same level of control with a biological macromolecule; this will require that the difficulties associated with maintaining a strong electrochemical coupling to the underlying electrode whilst simultaneously imaging at very high resolution, be addressed.

With recent significant advances in nanometer-resolved functional imaging, combined optical approaches and single molecule spectroscopic studies, the rapidly developing applicability of this technology to biological systems shows little sign of tailing off. As the sensitivity, feedback response rate and control of scanning probe systems improves, their ability to enhance our deepening understanding of biomolecular and cellular processes should continue at a rapid rate.

The authors are indebted to the efforts of a number of students and co-workers; Professors G. W. Canters, W. Maret and B. L. Vallee, Drs D. Bruce, K. K. W. Lo, E. N. K. Wallace and L.-L. Wong and Mr S. Myers and Ms D. Djuricic. The EPSRC, BBSRC, the EU, Abbott Inc., and Oxford Biosensors Ltd are thanked for financial help. J.J.D wishes to acknowledge the support of The Queen's College, Oxford and The Royal Society.

Notes and references

† One should note that, unlike AFM topographs (in the absence of compression), the height data in tunnelling images is 'false' in the sense that it is representative of a complex convolution of structural (topographic) and electronic contributions. Unless the electronic properties of an adsorbate (such as its nominal electron affinity/work function) closely mirrors that of the underlying substrate, this height deviates significantly from that which is purely topographic. In view of the characteristic low conductivity of biomolecules, the 'height' is almost without exception measured to be significantly less than observed by, for example, AFM or ellipsometric methods.

‡ http://www.nature.com/

1 A. E. G. Cass, G. Davis, G. D. Francis, H. A. O. Hill, W. J. Aston, I. J. Higgins, E. V. Plotkin, D. L. Scott and A. P. F. Turner, *Anal. Chem.*, 1984, **56**, 667.
2 G. J. Leggett, M. C. Davies, D. E. Jackson, C. J. Roberts, S. J. B. Tendler and P. M. Williams, *J. Phys. Chem.*, 1993, **97**, 8852.
3 N. Patel, M. C. Davies, M. Hartshorne, R. J. Heaton, C. J. Roberts, S. J. B. Tendler and P. M. Williams, *Langmuir*, 1997, **13**, 6485.
4 G. J. Leggett, C. J. Roberts, P. M. Williams, M. C. Davies, D. E. Jackson and S. J. B. Tendler, *Langmuir*, 1993, **9**, 2356.
5 S. N. Magonov and D. H. Reneker, *Ann. Rev. Mater. Sci.*, 1997, **27**, 125.
6 H. G. Hansma and J. H. Hoh, *Ann. Rev. Biophys. Biomol. Struct.*, 1994, **23**, 115.
7 S. N. Magonov, V. Elings and M. H. Whangbo, *Surf. Sci.*, 1997, **375**, L385.
8 M. H. Whangbo, G. Bar and R. Brandsch, *Surf. Sci.*, 1998, **411**, L794.
9 W. Han, S. M. Lindsay and T. Jing, *Appl. Phys. Lett.*, 1996, **69**, 4111.
10 W. Han, S. M. Lindsay, M. Dlakic and R. E. Harrington, *Nature*, 1997, **386**, 563.
11 R. Pethig, *Dielectric and Electronic Properties of Biological Materials*, Wiley, New York, 1979.
12 R. Guckenberger, B. Hacker, T. Hartmann, T. Scheybani, Z. Wang, W. Weigrabe and W. Baumeister, *J. Vac. Sci. Technol. B*, 1991, **9**(2), 1227.
13 C. Joachim and J. K. Gimzewski, *Europhys. Lett.*, 1995, **30**(7), 409.
14 D. M. Eigler, P. S. Weiss, E. K. Schweizer and N. D. Lang, *Phys. Rev. Lett.*, 1991, **66**, 1189.
15 J. K. Spong, H. A. Mizes, L. J. LaComb, M. M. Dovek, J. E. Frommer and J. S. Foster, *Nature*, 1989, **338**, 137.
16 S. M. Lindsay, T. W. Jing, J. Pan, A. Vaught and D. Rekesh, *Nanobiology*, 1994, **3**, 17.
17 E. P. Friis, Y. I. Kharkats, A. M. Kuznetsov and J. Ulstrup, *J. Phys. Chem. A*, 1998, **102**, 7851.
18 M. Amrein, R. Durr, A. Stasiak, H. Gross and G. Travaglini, *Science*, 1989, **243**, 1708.
19 R. Guckenberger, B. Hacker, T. Hartmann, T. Scheybani, Z. Wang, W. Weigrabe and W. Baumeister, *Ultramicroscopy*, 1989, **31**, 327.
20 A. M. Kuznetsov, P. Sommer-Larsen and J. Ulstrup, *Surf. Sci.*, 1992, **275**, 52.
21 S. M. Lindsay and O. F. Sankey, *Scanned Probe Microscopy*, ed. H. K. Wickramasinghe, New York, p. 235, 1992.
22 B. Zhang and E. Wang, *J. Chem. Soc., Faraday Trans.*, 1997, **93**(2), 327.
23 Z. F. Liu, A. Manivannan, H. Yanagi, M. Ashida, A. Fujishima and H. Inokucho, *Surf. Sci. Lett.*, 1993, **284**, L411.
24 R. D. Edstrom, M. H. Meinke, X. Yang, R. Yang and D. F. Evans, *Biochemistry*, 1989, **28**, 4939.
25 Q. Chi, J. Zhang, S. Dong and E. Wang, *J. Chem. Soc., Faraday Trans.*, 1994, **90**(14), 2057.
26 M. Parker, M. C. Davies and S. J. B. Tendler, *J. Phys. Chem.*, 1995, **99**, 16155.
27 J. J. Davis, C. M. Halliwell, H. A. O. Hill, G. W. Canters, M. C . van Amsterdam and M. P. Verbeet, *New J. Chem.*, 1998, 1119.
28 E. P. Friis, J. E. T. Andersen, Y. I. Kharkats, A. M. Kuznetsov, R. J. Nichols, J. D. Zhang and J. Ulstrup, *Proc. Natl. Acad. Sci. USA*, 1999, **96**, 1379.
29 J. D. Zhang, Q. Chi, S. J. Dong and E. Wang, *J. Electroanal. Chem.*, 1994, **379**, 535.
30 R. Mudhopakhyay, J. J. Davis, P. Kyritsis, H. A. O. Hill and J. Meyer, *J. Inorg. Biochem.*, 2000, **78**, 251.

31 J. J. Davis, H. A. O. Hill, A. Kurz, C. Jacob, W. Maret and B. L. Vallee, *Phys. Chem. Commun*., 1998, **1**, 12.
32 J. J. Davis, H. A. O. Hill and A. M. Bond, *Coord. Chem. Rev*., 2000, **200–202**, 411.
33 *Copper Proteins and Copper Enzymes, CRC Press, Boca Raton FL*, ed. R. Lontie, 1984, 1.
34 H. Nar, R. Huber, A. Messerschmidt, M. van der Kamp and G. W. Canters, *J. Mol. Biol*., 1991, **221**, 765.
35 T. J. White, N. Arnheim and H. A. Erlich, *Trends in Genetics*, 1989, **15**, 185.
36 G. W. Canters and G. Gilardi, *FEBS Lett*., 1993, **325**, 39.
37 P. Tengvall, M. Lestelius, B. Liedberg and I. Lundstrom, *Langmuir*, 1992, **8**, 1236.
38 A. Ihs and B. Liedberg, *J. Colloid Interfac. Sci*., 1991, **144**, 282.
39 M. J. S. Dewar, E. G. Zoebisch, E. F. Healy and J. J. P. Stewart, *J. Am. Chem. Soc*., 1985, **107**, 3902.
40 D. M. Cyr, B. Venkataraman, G. W. Flynn, A. Black and G. M. Whitesides, *J. Phys. Chem*., 1996, **100**, 13747.
41 Y. M. Lvov, Z. Lu, J. B. Schenkman, X. Zu and J. F. Rusling, *J. Am. Chem. Soc*., 1998, **120**, 4073.
42 K. K. W. Lo, L. L. Wong and H. A. O. Hill, *FEBS Lett*., 1999, **451**, 342.
43 P. S. Stayton and S. G. Sligar, *Biochemistry*, 1990, **29**, 7381.
44 T. L. Poulos, B. C. Finzel and A. J. Howard, *J. Mol. Biol*., 1987, **195**, 687.
45 C. A. Hasemann, R. G. Kurumbail, S. S. Boddupali, J. A. Peterson and J. Deisenhofer, *Structure*, 1995, **3**, 41.
46 R. Guckenberger, M. Heim, G. Cevc, H. F. Knapp, W. Weigrabe and A. Hillebrand, *Science*, 1994, **266**, 1538.
47 M. C. Parker, M. C. Davies and S. J. B. Tendler, *J. Vac. Sci. Technol. B*, 1996, **9**, 1227.
48 J. Y. Yuan, Z. Shao and C. Gao, *Phys. Rev. Lett*., 1991, **67**, 863.
49 D. J. Muller, F. A. Schabert, G. Buldt and A. Engel, *Biophys J*., 1995, **68**, 1681.
50 H. Seelert, A. Poetsch, N. A. Dencher, A. Engel, H. Stahlberg and D. J. Muller, *Nature*, 2000, **405**, 418.
51 A. Ishijima and T. Yanagida, *Trends Biochem. Sci*., 2001, **26**(7), 438.
52 P. Tamarat, A. Maali, B. Lounis and M. Orrit, *J. Phys. Chem. A*, 2000, **104**(1), 1.
53 A. K. Chamberlain, C. E. MacPhee, J. Zurdo, L. A. Morozova-Roche, H. A. O. Hill, C. M. Dobson and J. J. Davis, *Biophys. J*., 2000, **79**, 3282.
54 N. J. Tao, *Phys. Rev. Lett*., 1996, **76**(21), 4066.
55 H. J. Hecht, H. M. Kalisz, J. Hendle, R. D. Schmid and D. Schomburg, *J. Mol. Biol*., 1993, **229**, 153.
56 P. A. Williams, V. Fulop, E. F. Garman, N. F. Saunders, S. J. Ferguson and J. Hajdu, *Nature*, 1997, **389**, 406.